USGS
science for a changing world

U.S. DEPARTMENT OF THE INTERIOR
U.S. GEOLOGICAL SURVEY

Open-File Report 2010–1083-N

Seismicity of the Earth 1900–2012

Java and Vicinity

Compiled by Eric S. Jones,[1] Gavin P. Hayes,[1] Melissa Bernardino,[2] Fransiska K. Dannemann,[3] Kevin P. Furlong,[4] Harley M. Benz,[1] and Antonio Villaseñor[5]
2014

[1]U.S. Geological Survey
[2]Department of Geological Sciences, University of Colorado, Boulder, Colo., USA
[3]Department of Geological Sciences, Indiana University, Bloomington, Ind., USA
[4]Department of Geosciences, Pennsylvania State University, University Park, Pa., USA
[5]Institute of Earth Sciences, Consejo Superior de Investigaciones Científicas, (CSIC), Barcelona, Spain

TECTONIC SUMMARY

The Sunda convergent margin extends for 5,600 km from the Bay of Bengal and the Andaman Sea, both located northwest of the map area, towards the island of Sumba in the southeast, and then continues eastward as the Banda arc system. This tectonically active margin is a result of the India and Australia plates converging with and subducting beneath the Sunda plate at a rate of approximately 50 to 70 mm/yr. The main physiographic feature associated with this convergent margin is the Sunda-Java Trench, which stretches for 3,000 km parallel to the Java and Sumatra land masses and terminates at 120° E. The convergence of the Indo-Australia and Sunda plates produces two active volcanic arcs: Sunda, which extends from 105 to 122° E and Banda, which extends from 122 to 128° E. The Sunda arc results solely from relatively simple oceanic plate subduction, while the Banda arc represents the transition from oceanic subduction to continental collision, where a complex, broad deforming zone is found.

Based on modern activity, the Banda arc can be divided into three distinct zones: an inactive section, the Wetar Zone, bound by two active segments, the Flores Zone in the west and the Damar Zone in the east. The lack of volcanism in the Wetar Zone is attributed to the collision of Australia with the Sunda plate. The absence of gap in volcanic activity is underlain by a gap in intermediate depth seismicity, which is in contrast to nearly continuous, deep seismicity below all three sections of the arc. The Flores Zone is characterized by down-dip compression in the subducted slab at intermediate depths and late Quaternary uplift of the forearc. These unusual features, along with GPS data interpretations indicate that the Flores Zone marks the transition between subduction of oceanic crust in the west and the collision of continental crust in the east.

The Java section of the Sunda arc is considered relatively aseismic historically when compared to the highly seismically active Sumatra section, despite both areas being located along the same active subduction margin. Shallow (0–20 km) events have occurred historically in the overlying Sunda plate, causing damage to local and regional communities. A recent example was the May 26, 2006 M6.3 left-lateral strike-slip event that occurred at a depth of 10 km in central Java, and caused over 5,700 fatalities. Intermediate depth (70–300 km) earthquakes frequently occur beneath Java as a result of intraplate faulting within the Australia slab. Deep (300–650 km) earthquakes occur beneath the Java Sea and the back-arc region to the north of Java. Similar to other intermediate depth events, these earthquakes are also associated with intraslab faulting. However, this subduction zone exhibits a gap in seismicity from 250 to 400 km, interpreted as the transition between extensional and compressional slab stresses. Historical examples of large intraplate events include: the 1903 M8.1 event, 1921 M7.5 event, 1977 M8.3 event, and August 2007 M7.5 event.

Large thrust earthquakes close to the Java trench are typically interplate faulting events along the slab interface between the Australia and Sunda plates. These earthquakes also generally have high tsunamigenic potential due to their shallow hypocentral depths. In some cases, these events have demonstrated slow moment-release and have been defined as ‘tsunami’ earthquakes, where rupture is large in the weak crustal layers very close to the seafloor. These events are categorized by tsunamis that are significantly larger than predicted by the earthquake’s magnitude. The most notable tsunami earthquakes in the Java region occurred on June 2, 1994 (M7.8) and July 17, 2006 (M7.7). The 1994 event produced a tsunami with wave runup heights of 13 m, killing over 200 people. The 2006 event produced a tsunami of up to 15 m, and killed 730 people. Although both of these tsunami earthquakes were characterized by rupture along thrust faults, they were followed by an abundance of normal faulting aftershocks. These aftershocks are interpreted to result from extension within the subducting Australia plate, whereas the mainshocks represented interplate faulting between the Australia and Sunda plates.

Seismic Hazard and Relative Plate Motion

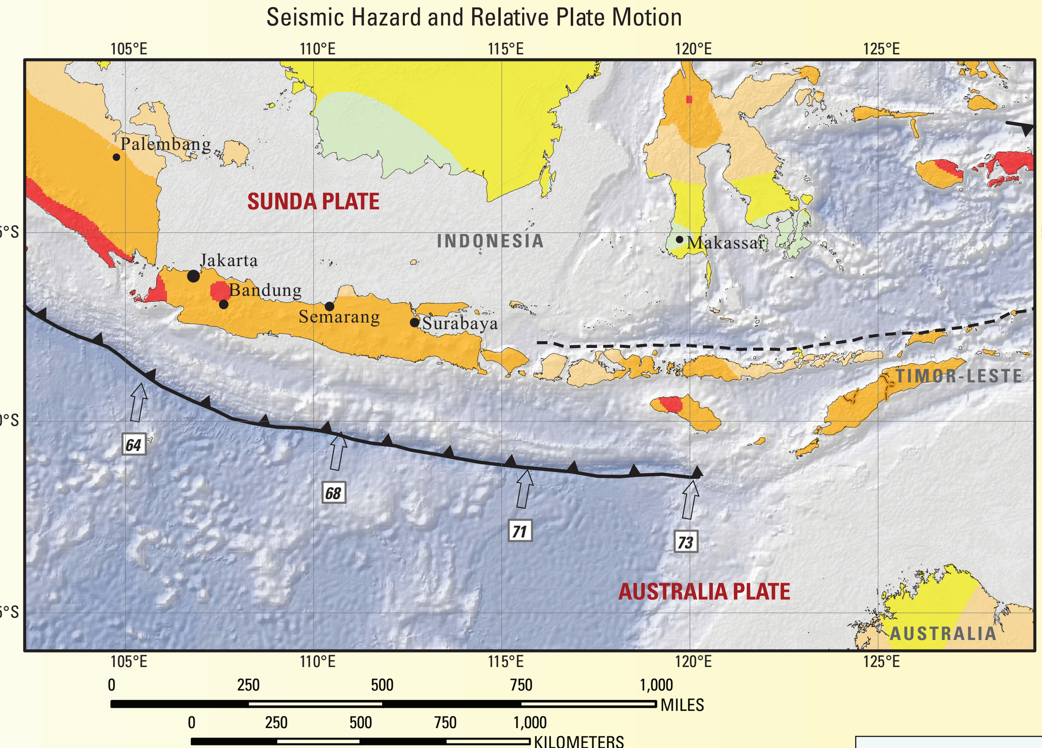

FIGURE EXPLANATION

Peak ground acceleration
0–0.2 m/s²
0.2–0.4
0.4–0.8
0.8–1.6
1.6–3.2
3.2–6.4
6.4–9.8

Plate motion in mm/yr (AUSTRALIA:SUNDA)
73

Plate boundaries
Subduction
Other

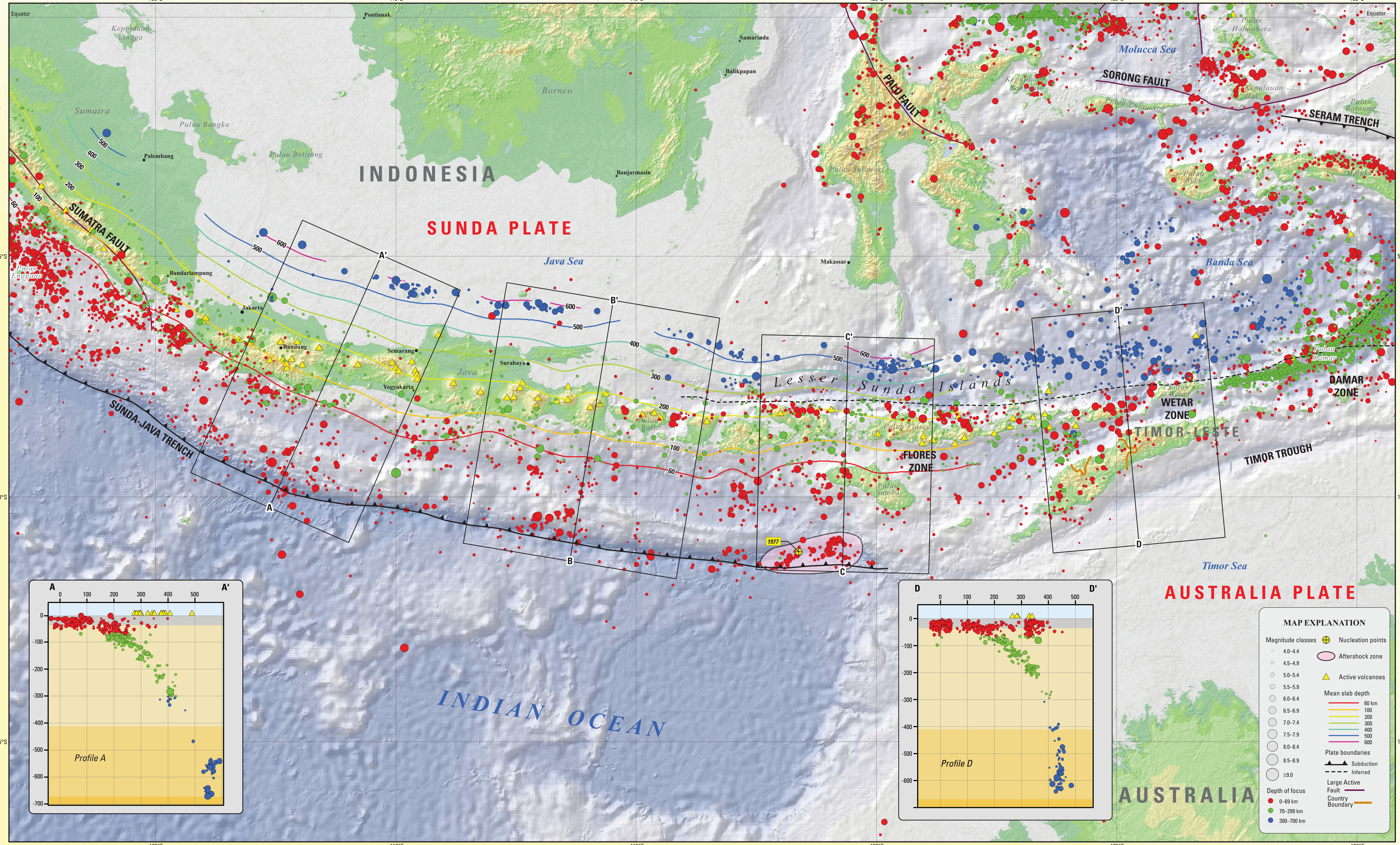

World Mercator Projection
Digital map database and cartography by Eric S. Jones

SCALE 1:5 000 000
0 100 200 300 400 500 MILES
0 100 200 300 400 500 KILOMETERS

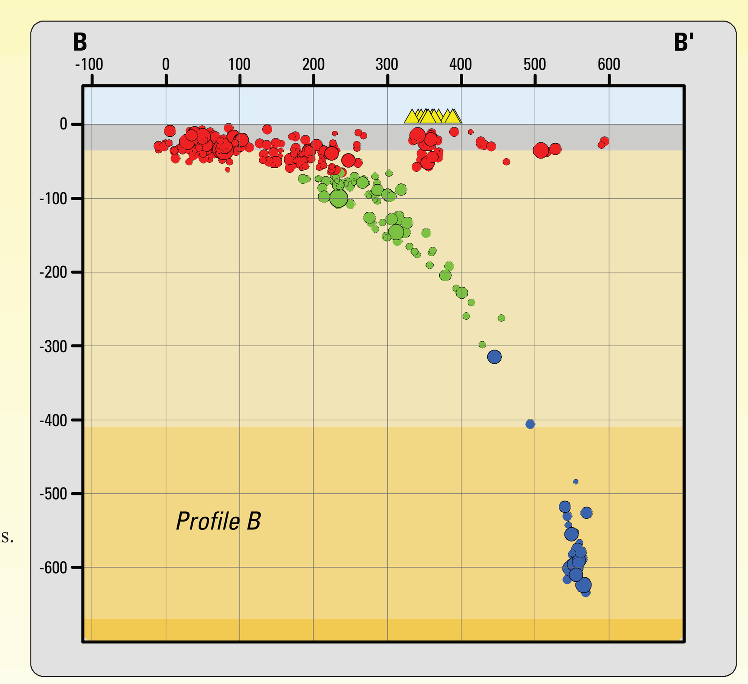

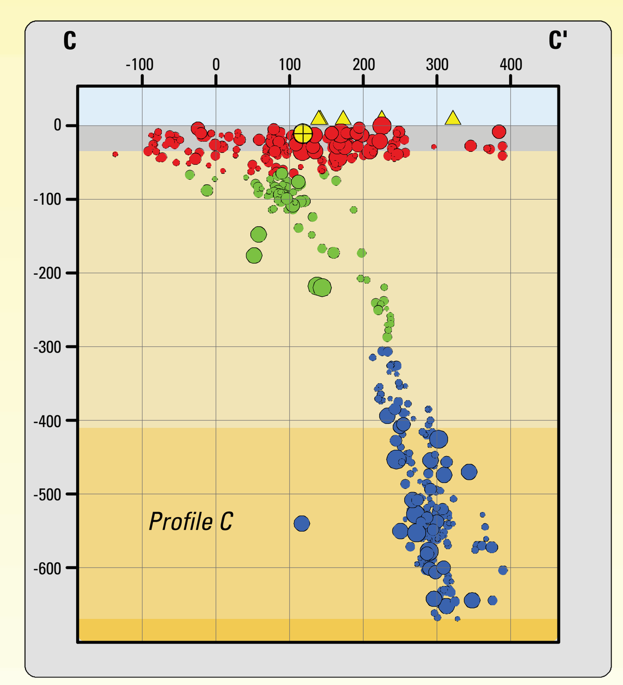

DEPTH PROFILE EXPLANATION

Magnitude classes: 4.0–4.4; 4.5–4.9; 5.0–5.4; 5.5–5.9; 6.0–6.4; 6.5–6.9; 7.0–7.4; 7.5–7.9; 8.0–8.4; 8.5–8.9; ≥9.0

Depth of focus: 0–69 km; 70–299 km; 300–700 km

Nucleation points of M>8.3 events

Active volcanoes

Earth structure: Air; Crust; Upper mantle; Transition zone; Lower mantle

Profiles of earthquake and volcano locations are constructed from the mapped data. Locations of the profile intersection with the surface are drawn in the map and labeled to coincide with the profile label. Box defines extent of earthquakes included in the profile. Length of the profile graphic is the same as in the map. Distance in kilometers from the trench axis or trough is indicated in the X direction, depth in kilometers in the Y direction. There is no vertical exaggeration. See explanation left for color key. Not all earth layers, earthquake depths or magnitude, are visible on every profile.

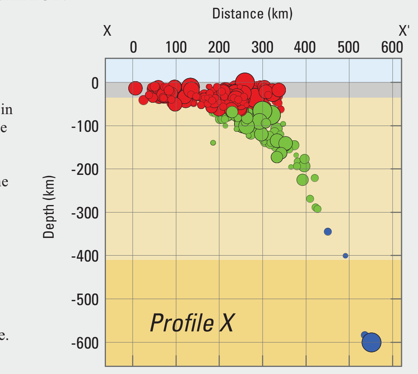

DATA SOURCES

The earthquakes portrayed on the main map (upper right) are taken from two sources: (a) the Centennial earthquake catalog (Engdahl and Villaseñor, 2002) and annual supplements for the interval 1900–2007, where the magnitude floor is 5.5 globally, and (b) the National Earthquake Information Center (NEIC) Preliminary Determination of Epicenters (PDE) Catalog M4.0 and larger from 1973 to July 2012.

1900–2001 Centennial Catalog M=5.5–9.5 (Engdahl and Villasenor, 2002)
2002–2012 NEIC Catalog M=5.5–9.2
1964–2001 EHB catalog M=4.0–5.4 (Engdahl, personal commun., 2003)
2002–2012 NEIC Catalog M<5.5

The nucleation points of great earthquakes (M≥8.3) are designated with a label showing the year of occurrence. Their aftershock zones are shown as pale-reddish polygons. Major earthquakes (7.5≤M≤8.2) are labeled with the year of occurrence.

The Seismic Hazard and Relative Plate Motion panel (left) displays the generalized seismic hazard of the region (Giardini and others, 1999) and representative relative plate motion vectors using the MORVEL model (DeMets and others, 2010.)

Pre-instrumental seismicity if shown, was obtained from the NOAA National Geophysical Data Center (2010) database of significant earthquakes; locations are approximate, based on macro-seismic reports and field investigations. We selected earthquakes with the associated reports of moderate to major damage, 10 or more deaths, an estimated magnitude of 7.5 or greater (if known), Modified Mercalli Intensities X, or tsunami generation.

Base map data sources include GEBCO 2008, Volcanoes of the World dataset (Siebert and Simkin, 2002), plate boundaries (Bird, 2003), Digital Chart of the World, and Esri. Slab contours are from Hayes and others (2012).

REFERENCES

Abercrombie, R.E., Antolik, Michael, Felzer, Karen, and Ekström, Göran, 2001, The 1994 Java tsunami earthquake—Slip over a subducting seamount: Journal of Geophysical Research, v. 106, p. 6595–6607.
Ammon, C.J., Kanamori, Hiroo, Lay, Thorne, and Velasco, A.A., 2006, The 17 July Java tsunami earthquake: Geophysical Research Letters, v. 33, L24308, doi: 10.1029/2006GL028005.
Bird, Peter, 2003, An updated digital model of plate boundaries: Geochemistry Geophysics Geosystems, v. 4, no. 3, 52 p.
DeMets, Charles, Gordon, R.G., and Argus, D.F., 2010, Geologically current plate motions: Geophysical Journal International, v. 181, p. 1–80, doi: 10.1111/j.1365-246X.2009.04491.x.
Earth Hazards Program—Slab Models for Subduction Zones: U.S. Geological Survey, accessed February 23, 2013, at *http://earthquake.usgs.gov/research/data/slab/*.
Engdahl, E.R., and Villaseñor, Antonio, 2002, Global seismicity: 1900–1999, *in* Lee, W.H.K., Kanamori, Hiroo, Jennings, P.C., and Kisslinger, Carl, eds., International Handbook of Earthquake and Engineering Seismology: San Diego, Calif., Academic Press, v. 81(A), chap. 41, p. 1–26.
Esri, 2002, Esri data and maps: Redlands, Calif., ESRI, *http://www.esri.com/data/data-maps*.
GEBCO, 2008, The GEBCO_08_Grid, ver. 20091120: GEBCO, accessed July 5, 2012, at *http://www.gebco.net*.
Giardini, Domenico, Grünthal, Gottfried, Shedlock, Kaye, Zhang, Peizhen, and Global Seismic Hazards Program, 1999, Global Seismic Hazards Map: Accessed January 9, 2007, at *http://www.seismo.ethz.ch/static/GSHAP/*.
Hayes, G.P., Wald, D.J. and Johnson, R.L., 2012, Slab 1.0—A three-dimensional model of global subduction zone geometries: Journal of Geophysical Research, v. 117, doi: 10.1029/2011JB008524.
Malod, J.A., Karta, Komar, Beslier, M.O., and Zen, M.T., Jr., 1995, From normal to oblique subduction—Tectonic relationships between Java and Sumatra: Journal of Southeast Asian Earth Sciences, v. 12, p. 85–93.
National Geospatial-Intelligence Agency (NGA), 1992, Digital Chart of the World: National Geospatial-Intelligence Agency, accessed March 9, 1996, at *http://earth-info.nga.mil/publications/specs/printed/89009/89009_DCW.pdf*.
National Oceanic and Atmospheric Administration (NOAA), 2010: National Geophysical Data Center (NGDC): National Oceanic and Atmospheric Administration, accessed on Mar. 31, 2010, at *http://www.ngdc.noaa.gov/hazard.html*.
Siebert, Lee, and Simkin, Thomas, 2002, Volcanoes of the world—An illustrated catalog of Holocene volcanoes and their eruptions: Smithsonian Institution, Global Volcanism Program Digital Information Series, GVP-3, accessed January 9, 2007, at *http://www.volcano.si.edu/world*.
Spence, William, 1986, The 1977 Sumba earthquake series—Evidence for slab pull force acting at a subduction zone: Journal of Geophysical Research, v. 91, no. 87, p. 7225–7239.
Tarr, A.C., Villaseñor, Antonio, Furlong, K.P., Rhea, Susan, and Benz, H.M., 2010, Seismicity of the Earth 1900–2007: U.S. Geological Survey Scientific Investigations Map 3064, scale 1:25,000,000.

This and other USGS information products are available at *http://store.usgs.gov/*
U.S. Geological Survey
Box 25286, Denver Federal Center
Denver, CO 80225

To learn about the USGS and its information products visit *http://www.usgs.gov/*
1-888-ASK-USGS

This report is available at:
http://pubs.usgs.gov/of/2010/1083/n

For more information concerning this publication, contact:
Center Director, USGS Geologic Hazards Science Center
Box 25046, Mail Stop 966
Denver, CO 80225
(303) 273-8579

Or visit Geologic Hazards Science Center Web site at:
http://geohazards.cr.usgs.gov/

Publishing support provided by:
Denver Publishing Service Center

Manuscript approved for publication May 19, 2014

Suggested citation:
Jones, E.S., Hayes, G.P., Bernardino, Melissa, Dannemann, F.K., Furlong, K.P., Benz, H.M., and Villaseñor, Antonio, 2014, Seismicity of the Earth 1900–2012 Java and vicinity: U.S. Geological Survey Open-File Report 2010–1083-N, 1 sheet, scale 1:5,000,000, *http://dx.doi.org/10.3133/ofr20101083N*.

ISSN 2331-1258 (online)